Rubber Co., R&D Division for the catalyst and high molecular weight PPO samples, and Dr. Leo Kadehjian for synthesis of the initiator dye. We also thank Dr. G. Ronca and Dr. G. Hadziioannou of IBM Research for helpful discussions.

References and Notes

(1) Edwards, S. F. In "Molecular Fluids"; Balian, R., Weill, G., Eds.; Gordon and Breach: London, 1976; pp 151–208.
(2) de Gennes, P.-G. "Scaling Concepts in Polymer Physics"; Cornell University Press: Ithaca, NY, 1979.
(3) Daoud, M.; de Gennes, P.-G. *J. Polym. Sci., Polym. Phys. Ed.* 1979, *17*, 1971–1981.
(4) Léger, L.; Hervet, H.; Rondelez, F. *Macromolecules* 1981, *14*, 1732.
(5) Klein, J. *Nature (London)* 1978, *271*, 143–145.
(6) Klein, J.; Briscoe, B. J. *Proc. R. Soc. London, A* 1979, *365*, 53–73.
(7) Smith, B. A.; Samulski, E. T.; Yu, L.-P.; Winnik, M. A. *Phys. Rev. Lett.* 1984, *52*, 45–48.
(8) Wendel, H.; Noolandi, J. *Macromolecules* 1982, *15*, 1318–1320.
(9) Smith, B. A. *Macromolecules* 1982, *15*, 469–472.
(10) Smith, B. A.; McConnell, H. M. *Proc. Natl. Acad. Sci. U.S.A.* 1978, *75*, 2759.
(11) Smith, L. M.; Smith, B. A.; McConnell, H. M. *Biochemistry* 1979, *18*, 2256.
(12) Livigni, R. A.; Herold, R. J.; Eliner, O. C.; Aggarwal, S. L. *ACS Symp. Ser.* 1975, No. 6, 20.
(13) Yu, L.-P. Ph.D. Dissertation, University of Connecticut, 1984.
(14) Scholtan, V. W.; Lie, S. Y. *Makromol. Chem.* 1967, *108*, 104.
(15) Van Krevelen, D. W. "Properties of Polymers", 2nd ed.; Elsevier: Amsterdam, 1976; p 339.
(16) Klein, J.; Briscoe, B. J. *Proc. R. Soc. London, A* 1979, *365*, 53.
(17) Ferry, J. D. "Viscoelastic Properties of Polymers", 2nd ed.; Wiley: New York, 1970.
(18) Brandrup, J., Immergut, E. H., Eds. "Polymer Handbook", 2nd ed.; Wiley: New York, 1975; p III–158.
(19) Kirkwood, J. G.; Riseman, J. *J. Chem. Phys.* 1948, *16*, 565–573.
(20) Debye, P.; Bueche, A. M. *J. Chem. Phys.* 1948, *16*, 573–579.
(21) Flory, P. *J. Chem. Phys.* 1949, *17*, 303–310.
(22) Graessley, W. W. *Adv. Polym. Sci.* 1982, *47*, 67–117.
(23) Tanner, J. E. *Macromolecules* 1971, *4*, 748–750.
(24) Klein, J. *Macromolecules* 1981, *14*, 460–461.
(25) Green, P. F.; Mills, P. J.; Palmstrom, C. J.; Mayer, J. W.; Kramer, E. J. *Phys. Rev. Lett.* 1984, *53*, 2145–2148.
(26) Graessley, W. W. *J. Polym. Sci., Polym. Phys. Ed.* 1980, *18*, 27–34.
(27) Brandrup, J., Immergut, E. H., Eds. "Polymer Handbook", 2nd ed.; Wiley: New York, 1975; p IV–45.

Normal Vibrational Analysis of Benzanilide. A Model for Poly(p-phenylene terephthalamide)

P. K. Kim and S. L. Hsu*

Polymer Science and Engineering Department, University of Massachusetts, Amherst, Massachusetts 01003

H. Ishida

Department of Macromolecular Science, Case Western Reserve University, Cleveland, Ohio 44106. Received January 16, 1985

ABSTRACT: Vibrational analysis has been carried out for benzanilide, a model compound of poly(p-phenylene terephthalamide). The normal coordinate analysis has been carried out by using a set of nonredundant symmetry coordinates to overcome the difficulties in defining the appropriate force field. Satisfactory assignments were made for the infrared and Raman spectra obtained.

Introduction

A significant number of studies have been directed toward understanding the structure–property relationships of high-modulus/high-strength fibers or films of rigid-rod polymers such as poly(p-phenylene terephthalamide) (PPTA).[1,2] The structure of this polymer is shown schematically below.
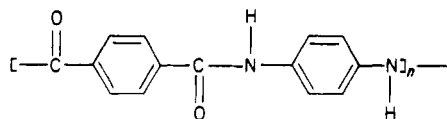
The molecular basis of the mechanical properties obtained for PPTA is largely due to the inherent chain stiffness and the high molecular structural order achieved during processing. For PPTA-like polymers, the formation of fibers or films involves several steps: (1) dissolution into strong acids such as 100% sulfuric acid with sufficiently high concentration to form an anisotropic liquid crystalline state, (2) extrusion of this anisotropic solution into a co-

**Table I
Structural Parameters of a Proposed Geometry of Benzanilide**

length, Å		valence angle, deg		dihedral angle, deg	
C–C	1.397	<(CCC)	120	τ(CCCC)	180
C–H	1.084	<(CCH)	120	τ(CCCH)	0
N–H	1.084	<(CCN)	120	$\tau(C_4C_5HN)$	30
C–N	1.42	<(CCC')	120	$\tau(C_4C_5NH)$	210
N–C'	1.34	<(CNH)	120	τ(HNC'O)	0
C'–O	1.24	<(CNC')	125	$\tau(NC'C_{16}C_{21})$	210
C'–C^a	1.47	<(CC'O)	120	$\tau(OC'C_{16}C_{21})$	30
		<(NC'C)	117		

^{a} C' = carbonyl carbon; C = ring carbon.

agulating bath, (3) neutralization and washing of the fibers and films, and (4) post-processing heat treatment.[3,4]

Therefore, information about the molecular structure in solution, polymer–solvent interaction, chain segment orientation, and the nature, specificity, or magnitude of the intermolecular interactions is important from both the practical and fundamental viewpoints. When bands are

* To whom correspondence should be addressed.

Table II
Definition of Internal Coordinates for Benzanilide

	atoms		atoms		atoms
$R_1 = r(C-H)$	(2,1)	$R_{34} = <(CCN)$	(4,5,10)	$R_{67} = <(CCC)$	(18,19,20)
$R_2 = r(C-H)$	(3,8)	$R_{35} = <(NCC)$	(10,5,6)	$R_{68} = <(CCC)$	(19,20,21)
$R_3 = r(C-H)$	(4,9)	$R_{36} = <(CCH)$	(5,6,11)	$R_{69} = <(CCC)$	(20,21,16)
$R_4 = r(C-N)$	(5,10)	$R_{37} = <(HCC)$	(11,6,7)	$R_{70} = CH$ opb^a	(2,1,7,3)
$R_5 = r(C-H)$	(6,11)	$R_{38} = <(CCH)$	(6,7,12)	$R_{71} = CH$ opb	(3,8,2,4)
$R_6 = r(C-H)$	(7,12)	$R_{39} = <(HCC)$	(12,7,2)	$R_{72} = CH$ opb	(4,9,3,5)
$R_7 = r(C-C)$	(2,3)	$R_{40} = <(CCC)$	(7,2,3)	$R_{73} = CN$ opb	(5,10,4,6)
$R_8 = r(C-C)$	(3,4)	$R_{41} = <(CCC)$	(2,3,4)	$R_{74} = CH$ opb	(6,11,5,7)
$R_9 = r(C-C)$	(4,5)	$R_{42} = <(CCC)$	(3,4,5)	$R_{75} = CH$ opb	(7,12,6,2)
$R_{10} = r(C-C)$	(5,6)	$R_{43} = <(CCC)$	(4,5,6)	$R_{76} = NH$ opb	(10,13,15,5)
$R_{11} = r(C-C)$	(6,7)	$R_{44} = <(CCC)$	(6,7,2)	$R_{77} = C'O$ opb	(15,14,16,10)
$R_{12} = r(C-C)$	(7,2)	$R_{45} = <(CCC)$	(6,7,2)	$R_{78} = CC'$ opb	(16,15,21,17)
$R_{13} = r(N-H)$	(10,13)	$R_{46} = <(CNH)$	(5,10,13)	$R_{79} = CH$ opb	(17,22,16,18)
$R_{14} = r(N-C')$	(10,15)	$R_{47} = <(HNC')$	(13,10,15)	$R_{80} = CH$ opb	(18,23,17,19)
$R_{15} = r(C'-O)$	(15,14)	$R_{48} = <(CNC')$	(5,10,15)	$R_{81} = CH$ opb	(19,24,18,20)
$R_{16} = r(C'-C)$	(15,16)	$R_{49} = <(NC'O)$	(10,15,14)	$R_{82} = CH$ opb	(20,25,19,21)
$R_{17} = r(C-H)$	(17,22)	$R_{50} = <(OC'C)$	(14,15,16)	$R_{83} = CH$ opb	(21,26,20,16)
$R_{18} = r(C-H)$	(18,23)	$R_{51} = <(NC'C)$	(10,15,16)	$R_{84} = C-C$ tor	(2,3)
$R_{19} = r(C-H)$	(19,24)	$R_{52} = <(CCC')$	(21,16,15)	$R_{85} = C-C$ tor	(3,4)
$R_{20} = r(C-H)$	(20,25)	$R_{53} = <(C'CC)$	(15,16,17)	$R_{86} = C-C$ tor	(4,5)
$R_{21} = r(C-H)$	(21,26)	$R_{54} = <(CCH)$	(16,17,22)	$R_{87} = C-C$ tor	(5,6)
$R_{22} = r(C-C)$	(16,17)	$R_{55} = <(HCC)$	(22,17,18)	$R_{88} = C-C$ tor	(6,7)
$R_{23} = r(C-C)$	(17,18)	$R_{56} = <(CCH)$	(17,18,23)	$R_{89} = C-C$ tor	(7,2)
$R_{24} = r(C-C)$	(18,19)	$R_{57} = <(HCC)$	(23,18,19)	$R_{90} = C-N$ tor	(10,5)
$R_{25} = r(C-C)$	(19,20)	$R_{58} = <(CCH)$	(18,19,20)	$R_{91} = N-C'$ tor	(15,10)
$R_{26} = r(C-C)$	(20,21)	$R_{59} = <(HCC)$	(24,19,20)	$R_{92} = C'-C$ tor	(16,15)
$R_{27} = r(C-C)$	(21,16)	$R_{60} = <(CCH)$	(20,21,26)	$R_{93} = C-C$ tor	(16,17)
$R_{28} = <(CCH)$	(7,2,1)	$R_{61} = <(HCC)$	(25,20,21)	$R_{94} = C-C$ tor	(17,18)
$R_{29} = <(HCC)$	(1,2,3)	$R_{62} = <(CCH)$	(20,21,26)	$R_{95} = C-C$ tor	(18,19)
$R_{30} = <(CCH)$	(2,3,8)	$R_{63} = <(HCC)$	(26,21,16)	$R_{96} = C-C$ tor	(19,20)
$R_{31} = <(HCC)$	(8,3,4)	$R_{64} = <(CCC)$	(21,16,17)	$R_{97} = C-C$ tor	(20,21)
$R_{32} = <(CCH)$	(3,4,9)	$R_{65} = <(CCC)$	(16,17,18)	$R_{98} = C-C$ tor	(21,16)
$R_{33} = <(HCC)$	(9,4,5)	$R_{66} = <(CCC)$	(17,18,19)		

^{a} opb definitions of the ring differ from those in ref 10 by a multiplication factor of sin (<CCC) (see text).

properly assigned, particularly when transition moments are well-defined, vibrational spectroscopy can be used to acquire the various microstructural information listed above. In addition, when reliable force constants are available, it is possible to calculate the theoretical mechanical properties[5,6] and to evaluate the stress-induced structural changes at the molecular level.[7] However, spectroscopic characterization of PPTA has been quite limited.[5,8,9] This has been due to the lack of both experimental data (to our knowledge there is no complete polarized infrared spectrum of Kevlar in published literature) and theoretical normal vibrational analysis of PPTA. The second cause is serious and is mainly due to the lack of a transferable force field. For complex molecules such as PPTA, a considerable number of branching and cyclic redundancies exist. Usually, in order to preserve the local symmetry of a molecule the internal coordinates containing these redundancies are used in the normal vibrational analysis. The number of force constants necessarily then increases, causing them to be nearly meaningless when transferred from one molecule to another. In other words, when redundant coordinates are used in the normal vibrational analysis, the force field becomes indeterminant. Without affecting the eigenvalues (frequencies) or eigenvectors (atomic displacements) calculated from secular equations, the force constants associated with redunant coordinates in a different set of potential energy fields are related to each other by an arbitrary constant. One should be extremely wary when transferring force fields from one molecule to another or in applying them to other types of calculations when the redundancy of the internal coordinates used has not been considered. For these reasons, we decided to carry out the normal vibrational analysis of PPTA and its model compound, benzanilide, with nonredundant coordinates only. The structure of the model compound is shown schematically below.
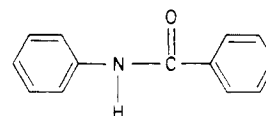
In this study we incorporated the approach of constructing the set of nonredundant coordinates for the benzene ring and the amide group separately before combining them. Therefore, the force constants can be derived from earlier theoretical studies on benzene[10] and polypeptide.[11] Normal vibrational analysis of these model compounds proved to be invaluable in the analysis of the polymer. Our methods and the results obtained for benzanilide are presented in this paper. The results of the polymer study will be given in a subsequent paper.

Normal Vibrational Analysis

Structure and Symmetry. The structure of PPTA has been derived from X-ray diffraction studies.[12] The structure deduced is in agreement with theoretical conformational analysis of a single chain.[5] Since there is little possibility for rotations around the virtual bond (C(= O)—N) to occur, PPTA has very low chain flexibility. Only minor differences exist between the benzene and amide structures from which the force constants were refined and the measured ones used in our calculation.

The exact structure of the model compound, benzanilide, has been given by Kashino and his co-workers.[13] It has a nonpolar configuration with a dihedral angle of approximately 30° between the benzene ring and the amide plane, similar to the measured PPTA structure.[12] These internal dihedral angles were deduced by considering the resonance effect trying to stabilize coplanarity of the amide

Table III
Definition of Local Nonredundant Symmetry Coordinates for Benzanilide

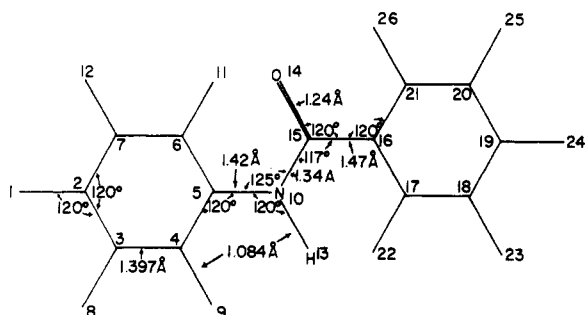|	notation	ring A	ring B
		Ring	
C–H str	r	$S_1 = R_1$	$S_{31} = R_{17}$
C–H str		$S_2 = R_2$	$S_{32} = R_{18}$
C–H str		$S_3 = R_3$	$S_{33} = R_{19}$
C–H str		$S_4 = R_5$	$S_{34} = R_{20}$
C–H str		$S_5 = R_6$	$S_{35} = R_{21}$
C–N str	R'	$S_6 = R_4$	
C–C' str	R''		$S_{36} = R_{16}$
C–C str	R	$S_7 = R_7$	$S_{37} = R_{22}$
C–C str		$S_8 = R_8$	$S_{38} = R_{23}$
C–C str		$S_9 = R_9$	$S_{39} = R_{24}$
C–C str		$S_{10} = R_{10}$	$S_{40} = R_{25}$
C–C str		$S_{11} = R_{11}$	$S_{41} = R_{26}$
C–C str		$S_{12} = R_{12}$	$S_{42} = R_{27}$
CH ipb	β	$S_{13} = (R_{29} - R_{28})/2^{1/2}$	$S_{43} = (R_{55} - R_{54})/2^{1/2}$
CH ipb		$S_{14} = (R_{31} - R_{30})/2^{1/2}$	$S_{44} = (R_{57} - R_{56})/2^{1/2}$
CH ipb		$S_{15} = (R_{33} - R_{32})/2^{1/2}$	$S_{45} = (R_{59} - R_{58})/2^{1/2}$
CH ipb		$S_{16} = (R_{37} - R_{36})/2^{1/2}$	$S_{46} = (R_{61} - R_{60})/2^{1/2}$
CH ipb		$S_{17} = (R_{39} - R_{38})/2^{1/2}$	$S_{47} = (R_{63} - R_{62})/2^{1/2}$
CN ipb	β'	$S_{18} = (R_{35} - R_{34})/2^{1/2}$	
CC' ipb	β''		$S_{48} = (R_{53} - R_{52})/2^{1/2}$
trigonal def.	q_{19}	$S_{19} = (R_{40} - R_{41} + R_{42} - R_{43} + R_{44} - R_{45})/6^{1/2}$	$S_{49} = (R_{64} - R_{65} + R_{66} - R_{67} + R_{68} - R_{69})/6^{1/2}$
asy def	q_{20}	$S_{20} = (2R_{40} - R_{41} - R_{42} + 2R_{43} - R_{44} - R_{45})/12^{1/2}$	$S_{50} = (2R_{64} - R_{65} - R_{66} + 2R_{67} - R_{68} - R_{69})/12^{1/2}$
asy def'	q_{21}	$S_{21} = (R_{41} - R_{42} + R_{44} - R_{45})/2$	$S_{51} = (R_{65} - R_{66} + R_{68} - R_{69})/2$
CH opb	γ	$S_{22} = R_{70}$	$S_{52} = R_{79}$
CH opb		$S_{23} = R_{71}$	$S_{53} = R_{80}$
CH opb		$S_{24} = R_{72}$	$S_{54} = R_{81}$
CH opb		$S_{25} = R_{74}$	$S_{55} = R_{82}$
CH opb		$S_{26} = R_{75}$	$S_{56} = R_{83}$
CN opb	γ'	$S_{27} = R_{73}$	
CC' opb	γ''		$S_{57} = R_{78}$
puckering	q_{28}	$S_{28} = (R_{84} - R_{85} + R_{86} - R_{87} + R_{88} - R_{89})/6^{1/2}$	$S_{58} = (R_{93} - R_{94} + R_{95} - R_{96} + R_{97} - R_{98})/6^{1/2}$
asy tor	q_{29}	$S_{29} = (-R_{84} + R_{86} - R_{87} + R_{89})/2$	$S_{59} = (-R_{93} + R_{95} - R_{96} + R_{98})/2$
asy tor'	q_{30}	$S_{30} = (-R_{84} + 2R_{85} - R_{86} - R_{87} + 2R_{88} - R_{89})/12^{1/2}$	$S_{60} = (-R_{93} + 2R_{94} - R_{95} - R_{96} + 2R_{97} - R_{98})/12^{1/2}$
		Amide Group	
N–H str	t	$S_{61} = R_{13}$	
N–C' str	R'	$S_{62} = R_{14}$	
C'–O str	S	$S_{63} = R_{15}$	
NH ipb	θ	$S_{64} = (R_{47} - R_{46})/2^{1/2}$	
<CNC' def	δ	$S_{65} = (2R_{48} - R_{47} - R_{46})/6^{1/2}$	
C'O ipb	θ'	$S_{66} = (R_{50} - R_{49})/2^{1/2}$	
<NC'C def	δ'	$S_{67} = (2R_{51} - R_{50} - R_{49})/6^{1/2}$	
NH opb	μ	$S_{68} = R_{76}$	
C'O opb	μ'	$S_{69} = R_{77}$	
C–N tor	τ_1	$S_{70} = R_{90}$	
N–C' tor	τ_2	$S_{71} = R_{91}$	
C'–C tor	τ_3	$S_{72} = R_{92}$	

Figure 1. Schematic structure of benzanilide.

group and the benzene rings and the counteracting steric hindrance found between the oxygen and ortho hydrogen of the adjacent benzene ring and between the amide hydrogen and ortho hydrogen of the other ring.[5] The structural parameters for benzanilide used in our analysis are listed in Table I. The structural parameters are also shown in Figure 1.

As mentioned earlier, for convenience or preservation of molecular local symmetry, experimental force fields are often expressed by including redundant coordinates in the
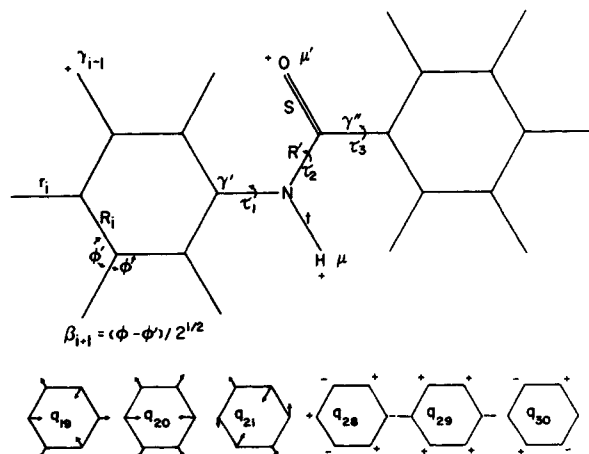

Figure 2. Definition of some of the nonredundant coordinates.

normal vibrational analysis. This procedure causes physically identical force fields to assume different numerical forms in different redundant coordinates. Another aspect of redundancy is the introduction of such high correlations between force constants of some internal co-
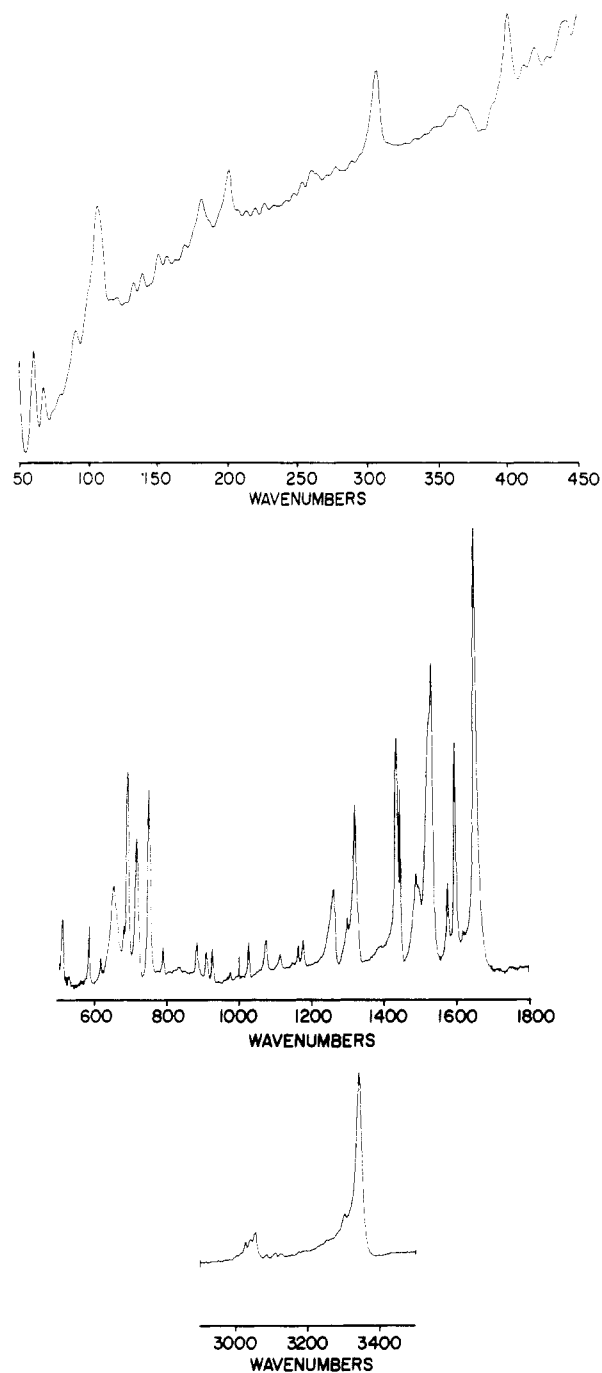
Figure 3. Infrared spectra of benzanilide. Resolution 2 cm^{-1}; 500 scans. (top) 50–450-cm^{-1} region, far-IR data; (middle) 500–1800-cm^{-1} region; (bottom) 2900–3500-cm^{-1} region.

Table IV
Force Constants for Benzanilide

force constant	value	force constant	value
Phenyl Group			
$K(r)$	5.104	$F(R)^{\circ}$	0.633
$K(r')$	5.043	$F(R)^{m}$	-0.442
$K(r'')$	4.409	$F(R)^{p}$	0.440
$K(R)$	6.500	$F(R_1\beta_1)$	0.167
$K(\beta)$	0.512	$F(R_1\beta_3)$	-0.010
$H(\beta')$	0.8375	$F(R_1\beta_4)$	0.019
$H(\beta'')$	0.8375	$F(R_1q_{20})$	0.134
$H(q_{19})$	1.236	$F(R_2q_{20})$	-0.268
$H(q_{20})$	1.236	$F(R_3q_{20})$	-0.067
$H(q_{20})$	1.236	$F(R_1q_{21})$	0.2321
$H(\gamma)$	0.5852	$F(R_3q_{21})$	-0.2321
$H(\gamma')$	0.6581	$F(\beta)^{\circ}$	0.009
$H(\gamma'')$	0.6581	$F(\beta)^{m}$	0.010
$H(q_{28})$	0.3763	$F(\beta)^{p}$	-0.001
$H(q_{29})$	0.3156	$F(\beta_2q_{20})$	-0.067
$H(q_{30})$	0.3156	$F(\beta_1q_{21})$	0.07736
$F(r)^{\circ}$	0.016	$F(\beta_2q_{21})$	-0.03863
$F(r)^{m}$	0.005	$F(\gamma)^{\circ}$	-0.092
$F(r)^{p}$	0.001	$F(\gamma)^{m}$	-0.0004
$F(r_1R_1)$	0.079	$F(\gamma)^{p}$	-0.0235
$F(r_1R_2)$	-0.002	$F(\gamma_1q_{28})$	-0.1681
$F(r_1R_3)$	-0.022	$F(\gamma_2q_{28})$	0.1681
$F(r_1\beta_2)$	0.005	$F(\gamma_1q_{29})$	0.1700
$F(r_1\beta_3)$	-0.007	$F(\gamma_2q_{29})$	-0.0850
$F(r_1q_{19})$	-0.105	$F(\gamma_2q_{30})$	-0.1472
$F(r_2q_{19})$	0.105	$F(\gamma_3q_{30})$	0.1472
$F(r_1q_{20})$	-0.099	$F(r'R_1)$	0.3
$F(r_2q_{20})$	0.0495	$F(r''R_1)$	0.2506
$F(r_2q_{21})$	-0.08574	$F(R_1\beta_1')$	0.220
$F(r_3q_{21})$	0.08574	$F(R_1\beta'')$	0.220
Amide Group			
$K(t)$	6.168	$F(R'\theta')$	-0.1414
$K(R')$	6.415	$F(R'\delta)$	0.1249
$K(S)$	9.582	$F(R'\delta')$	0.1633
$H(\theta)$	0.6205	$F(S\delta')$	-0.4899
$H(\delta)$	0.6625	$F(R''\theta')$	0.1414
$H(\theta')$	1.246	$F(r''\delta')$	0.1633
$H(\delta')$	1.3487	$F(r'\theta)$	-0.2079
$H(\mu)$	0.129	$F(r'\delta')$	0.1249
$H(\mu')$	0.587	$F(\theta\theta')$	-0.1255
$H(\tau_1)$	0.010	$F(\delta\delta')$	-0.0248
$H(\tau_2)$	0.680	$F(\theta'\delta)$	0.0725
$H(\tau_3)$	0.010	$F(\theta\delta')$	0.043
$F(\gamma'R')$	0.300	$F(\theta\delta)$	0.0231
$F(R'S)$	0.500	$F(\mu\mu')$	0.010
$F(r''R')$	0.300	$F(\mu'\tau_2)$	0.011
$F(r''S)$	0.500	$F(\mu\tau_2)$	-0.1677
$F(R'\theta)$	0.2079		

ordinates, making the refinement of force fields difficult, or even worse, meaningless. For these reasons, the use of redundant coordinates actually causes the resultant force fields to be less transferable among related molecules. This problem of redundancy is particularly serious for PPTA and its model compounds because, in addition to branching redundancies, cyclic redundancies exist for the benzene rings. This cyclic redundancy condition introduces very high correlations among the internal coordinates involved and, consequently, among the force constants for the benzene rings. In order to simplify our normal vibrational analysis, we decided to analyze benzanilide in parts by separating it into two monosubstituted benzene rings and an amide group, –CONH–, and PPTA by separating it into two disubstituted benzene rings and two amide groups. Furthermore, all calculations are based on individual sets

of nonredundant coordinates. This procedure greatly simplifies the vibrational analysis in two ways: first, the force field and the associated coordinates for each part are readily available from previous calculations and, second, the identification of the normal vibrations is much more easily accomplished.

In general there are two methods to obtain nonredundant coordinates for a complex molecule with low symmetry. The first method is quite suitable for computer calculations, and this has been proposed by Gussoni and Zerbi.[14] Because of the redundancy condition, the dynamic matrix, G, is a singular matrix. Then all redundant internal coordinates can be identified by finding the eigenvectors that belong to zero eigenvalues of G. When these redundant coordinates are available, other desired nonredundant orthonormal coordinates are obtained by using the Gram–Schmidt orthogonalization process. The advantage of this method is that the whole procedure can be done by computer, and this can be applied regardless of the complexity of the molecule and the number and type of redundancies. The major disadvantage is that these nonredundant coordinates formed may have considerable
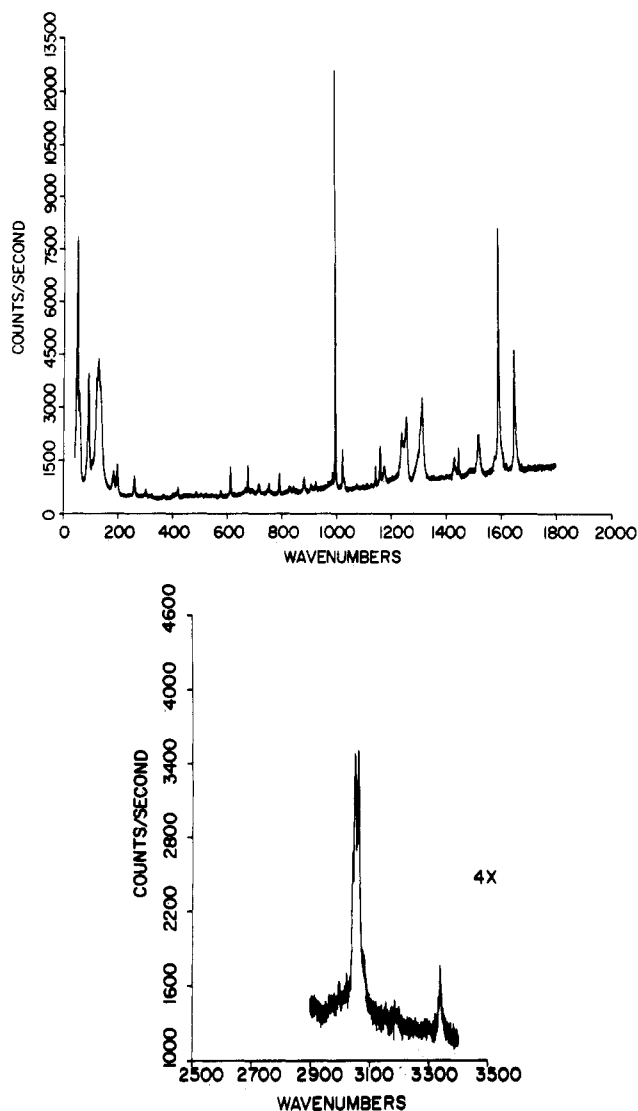
Figure 4. Raman spectra of benzanilide. Incident excitation radiation 5145 Å; 2-cm^{-1} bandpass at 5100 Å. (top) 0–1800-cm^{-1} region; (bottom) 2900–3400-cm^{-1} region.

stretchings, 18 angle bendings, 6 torsions, and 6 out-of-plane bendings. When the 12 redundancies (6 branching and 6 cyclic) are subtracted from the total number of internal coordinates, there should be 30 nonredundant coordinates as expected. These are listed in Table III. The definitions of each coordinate are the same as those in ref 10 except for the out-of-plane bending coordinates, for which the definition by Abe and Krimm[16] is used.

For the amide group, two branching redundancies are removed by the use of local symmetry coordinates as described above. The convention for the in-plane bending, out-of-plane bending, and torsion coordinates of the amide group have been defined by Abe and Krimm previously.[16] Only skeletal atoms of the amide group are used for the three torsion coordinates between the two rings.

In summary, 98 internal coordinates can be used to describe vibrational motions of benzanilide, but only 72 normal vibrations should exist. The 26 redundancies consist of 2 from the amide group and 24 from the two monosubstituted benzene rings. The complete set of internal coordinates and the associated nonredundant coordinates used for our benzanilide analysis are listed in Tables II and III. The definitions of the nonredundant coordinates are also shown schematically in Figure 2.

Force Field. In our analysis, the force field associated with benzene rings was obtained from Pulay and co-workers.[10] This set was chosen since it is most complete. These values are based on ab initio calculations and agree quite well for the ones refined to a series of benzene.[17] The force-constant changes needed for benzanilide, due to the differences between CC(O) and CN bonds connecting the amide group to each benzene ring, were quite minor. Force constants involving the stretching, in-plane bending, and out-of-plane bending modes of these connecting bonds were taken from the corresponding values for monosubstituted benzene rings.[17] The force constants for the amide group have been transferred from the work by Dwivedi and Krimm for a series of polypeptides.[11] The entire set of force constants are listed in Table IV. All normal vibrational analyses were performed by using Wilson's GF matrices with a set of programs modified from the earlier ones by Schachtschneider and Snyder.[18]

Experimental Section

The benzanilide used in this study was purchased from Aldrich Chemical Co. and recrystallized in EtOH three times. Deuterated benzanilide was prepared by placing the purified benzanilide into a small glass vial. The platelet crystals were heated until completely melted. A few drops of D_2O were added to the hot glass vial, immediately saturating the container. The container was then cooled in order to recrystallize the model compound. This simple procedure resulted in more than 90% deuteration. Since only one exchange site exists, i.e., the secondary amine group of the amide, no complications such as NHD groups arise. Spectral subtraction by FTIR or computerized Raman spectrometers yielded well-separated deuterated species without interference from the protonated species.

Infrared spectra were obtained for samples in potassium bromide. In each case, very high signal to noise ratios were obtained by using an International Business Machine Model 98 spectrometer. Raman spectra of benzanilide and its EtOH solution were taken with a Jobin-Yvon HG.2S spectrometer. This instrument can be controlled by a Cromenco System III computer. The data are then transferred to the Fourier transform instrument for further analysis.

The infrared and Raman spectra of benzanilide are shown in Figures 3 and 4, respectively. The Raman spectrum of benzanilide in solution is shown in Figure 5. The difference infrared and Raman spectra obtained for the deuterated molecule are shown in Figure 6.

mixing of internal coordinates, making the vibrational motions too complicated to recognize. A second method, which may not be generally applicable to all molecules, involves locating the local redundancies and then removing them by using local symmetry coordinates.[15] Therefore, one can overcome the disadvantage of the first method by selecting the proper linear combinations of internal coordinates so that each constructed nonredundant symmetry coordinate will be easier to visualize. We adapted this method in our analysis.

For the benzene ring, branching redundancies can easily be removed by using the local symmetry coordinates

$$S_1 = 2^{-1/2}(\Delta\phi_1 - \Delta\phi_2) \qquad (1)$$

$$S_2 = 6^{-1/2}(2\Delta\phi_3 - \Delta\phi_1 - \Delta\phi_2) \qquad (2)$$

where $\Delta\phi_1$, $\Delta\phi_2$, and $\Delta\phi_3$ are the changes in the valence angles around each carbon of the benzene ring. The additional six cyclic redundancies for each phenyl ring are more difficult to remove since there is no unique set of nonredundant coordinates. Therefore, it is advantageous to choose a set that describes the vibrational motions of the molecule most clearly. For benzene, we adopted the set described by Pulay et al.[10] Each monosubstituted benzene ring has 42 internal coordinates, including 12 bond

Table V (Continued)

IR	Raman	calcd	potential energy distribution[a]
			–NDCO–
	3070	3070	1A(11), 1B(88)
		3070	1A(88), 1B(11)
		3059	1A(89), 1B(10)
		3059	1A(10), 1B(89)
3050	3050	3049	1A(15), 1B(85)
		3049	1A(85), 1B(15)
		3040	1A(97)
3035		3032	1A(92), 1B(9)
		3032	1A(92), 1B(9)
2475		2462	12(97)
1647	1646	1654	18(19), 19(61), 22(12), 2B(13), 15(5)
	1596	1596	2A(9), 19(6), 14(10), 20(60), 3B(15), 5B(8)
1598		1593	11(5), 2A(67), 3A(15), 5A(7), 28(13)
		1585	2A(78), 3A(22), 6A(8)
1579		1577	19(8), 2B(70), 3B(22), 6B(6)
1502		1511	11(5), 2A(12), 3A(14), 18(9), 14(9), 2B(23), 3B(26)
1490	1495	1498	2A(24), 3A(41), 2B(12), 3B(20)
1465	1463	1460	2A(9), 3A(16), 18(10), 2B(13), 3B(28)
1449	1448	1449	2A(24), 3A(42), 2B(10), 3B(18)
1439		1437	2A(5), 3A(11), 18(14), 2B(20), 3B(38)
1400	1400	1319	2A(6), 3A(58), 3B(28)
1317	1317	1315	3A(31), 2B(5), 3B(59)
1300	1300	1287	2B(141), 3B(26)
		1285	2A(146), 3A(26)
1240		1236	11(32), 2A(14), 3A(12), 4A(10), 14(12), 2B(13), 3B(6)
1180		1180	3A(28), 2B(5), 3B(56)
		1179	2A(6), 3A(55), 3B(28)
1165	1165	1163	2A(6), 3A(18), 2B(18), 3B(53)
		1162	2A(18), 3A(55), 2B(6), 3B(19)
1138	1138	1137	2A(9), 4A(5), 18(7), 25(12), 14(12), 2B(18), 3B(9), 4B(13)
1077		1071	2A(34), 3A(24), 2B(14), 3B(10)
		1069	2A(14), 3A(9), 2B(36), 3B(24)
1029	1027	1019	2A(30), 3A(10), 4A(10), 2B(22), 3B(75), 4B(7)
		1017	2A(21), 3A(7), 4A(10), 2B(28), 3B(9), 4B(13)
1002	1000	985	2A(6), 4A(7), 2B(42)
980	985	985	2A(41), 4A(38), 2B(7), 4B(6)
		982	7A(94), 8A(22), 7B(41), 5B(10)
		982	7A(40), 8A(9), 7B(95), 8B(21)
		963	7A(110), 10A(10), 7B(16)
		963	7A(16), 7B(110), 10B(10)
		959	7A(7), 18(5), 23(7), 25(59), 2B(13)
927		925	7A(41), 13(7), 8A(8), 9A(5), 16(10), 7B(57), 8B(11), 9B(7)
907		910	7A(60), 8A(6), 7B(54), 8B(5)
875		857	7A(12), 18(11), 19(8), 22(12), 23(8), 24(14)
		838	7A(86), 7B(27)
		820	7A(6), 8A(9), 23(7), 27(10), 16(13), 7B(16), 8B(20)
790	794	785	11(14), 2A(23), 4A(11), 5A(14), 7A(5), 8A(7)
750		773	7A(24), 13(17), 8A(33), 21(15), 16(14), 7B(19), 8B(23)
711		698	7A(31), 7B(65), 8B(42)
		695	7A(64), 8A(55), 7B(9), 8B(23)
690		689	7A(9), 20(5), 21(32), 5B(12), 7B(35)
679	680	672	5A(5), 7A(5), 8A(12), 21(11), 23(8), 2B(7), 5B(35), 7B(7), 8B(13)
		629	7A(19), 8A(49), 20(5), 27(13), 6B(7), 7B(12), 8B(36)
		624	6B(72), 8B(7)
616	617	620	6A(80), 6B(6)
577		567	5A(38), 22(16), 23(7), 2B(6), 8B(7)
480		486	5A(13), 13(13), 9A(24), 5B(10), 16(14), 9B(29)
	422	422	5A(6), 7A(7), 13(21), 9A(91), 20(5), 23(6), 5B(5)
		403	16(5), 7B(22), 9B(18), 10B(117)
401		401	7A(28), 10A(157)
		398	12(7), 21(5), 22(5), 5B(5), 16(16), 7B(13), 9B(58), 10B(42)
	307	312	12(21), 9A(15), 23(28), 24(12), 14(5), 15(5), 5B(5)
	262	258	11(8), 12(10), 5A(7), 9A(5), 18(6), 14(11), 15(15), 5B(8), 9B(7)
	200	184	12(9), 7A(6), 13(12), 9A(15), 20(64), 24(6), 27(21)
	185	176	13(5), 9A(8), 21(10), 22(7), 15(23), 16(10), 7B(7), 9B(19)
	135	147	12(9), 20(14), 22(8), 24(11), 27(12), 15(11), 16(15), 7B(5), 9B(8)
	92	78	13(8), 9A(5), 20(20), 26(33), 27(29), 28(10), 16(9)
	62	65	12(15), 22(16), 24(36), 27(5), 15(7), 16(14)
	50	51	13(15), 20(12), 26(12), 27(34), 28(41)
		32	13(5), 26(47), 27(5), 28(41), 16(5)

[a] Number of the coordinate is followed by the potential energy in percent. Contributions less than 5% are not included. The coordinate definitions in potential energy distribution are (1) ring CH stretching; (2) ring CC stretching; (3) ring CH in-plane bending; (4) ring trigonal deformation; (5) ring asymmetric deformation, type 1 (q_{20}); (6) ring asymmetric deformation, type 1 (q_{21}); (7) ring CH out-of-plant bending; (8) ring puckering; (9) ring asymmetric torsion, type 1 (q_{29}); (10) ring asymmetric torsion, type 2 (q_{30}); (11) CN stretching; (12) CN in-plane bending; (13) CN out-of-plane bending; (14) C'C stretching; (15) C'C in-plane bending; (16) C'C out-of-plane bending; (17) NH(D) stretching; (18) NC' stretching; (19) C'=O stretching; (20) NH(D) out-of-plane bending; (21) C'=O out-of-plane bending; (22) NC'C bending; (23) C'=O in-plane bending; (24) CNC' bending; (25) NH(D) in-plane bending; (26) CN torsion; (27) NC' torsion; (28) C'C torsion.

Table V
Observed and Calculated Frequencies (in cm⁻¹) of Benzanilide

| IR	Raman	calcd	potential energy distribution[a]
			−NHCO−
3345	3342	3344	17(100)
	3070	3070	1B(94)
		3070	1A(94)
3055	3056	3059	1B(97)
		3059	1A(97)
	3049	3049	1B(100)
		3049	1A(100)
3041		3040	1B(100)
		3040	1A(100)
3027		3032	1B(75), 1A(26)
		3032	1A(75), 1B(26)
1656	1658	1657	19(62), 18(18), 22(13), 28(11), 15(5)
1600	1600	1606	2B(25), 19(7), 25(13), 14(10), 2B(31), 3B(7)
		1594	2A(48), 3A(10), 2B(32), 3B(7)
	1583	1587	2A(73), 3A(21), 5A(6)
	1579	1577	19(7), 2B(71), 3B(22), 6B(6)
1536	1524	1537	2A(12), 3A(6), 18(18), 23(6), 25(27), 14(7), 2B(20), 3B(9)
1502		1499	2A(31), 3A(52), 2B(5), 3B(9)
1493	1495	1489	2A(6), 3A(10), 25(10), 2B(24), 3B(49)
1449	1453	1449	2A(23), 3A(40), 2B(11), 3B(20)
1440	1437	1442	2A(9), 3A(17), 2B(23), 3B(43)
1329		1329	2A(9), 3A(44), 25(13), 14(8), 3B(18)
	1317	1315	3A(22), 2B(6), 3B(69)
1301	1300	1304	2A(67), 3A(40), 25(11), 3B(6)
		1288	2B(139), 3B(27)
1262	1260	1259	12(8), 2A(79), 3A(17), 25(17)
	1244	1234	12(27), 2A(16), 3A(10), 14(16), 2B(15), 3B(7)
1180	1179	1179	2B(8), 3B(82)
		1179	2A(9), 2B(80)
1166	1164	1162	3A(10), 2B(21), 3B(63)
		1162	2A(21), 3A(63), 3B(10)
1116	1113	1096	18(16), 19(7), 25(6), 2B(22), 3B(9), 4B(13)
1076	1079	1071	2A(47), 3A(33)
		1068	2B(43), 3B(31)
1028	1027	1019	2A(45), 3A(15), 4A(16), 2B(4)
		1016	2A(6), 2B(40), 3B(13), 4B(24)
1001	999	985	2A(36), 4A(37), 2B(9), 4B(10)
	991	984	2A(10), 4A(8), 2B(40), 4B(32)
979		982	7A(85), 8A(20), 7B(50), 8B(12)
		982	7A(51), 8A(11), 7B(86), 8B(19)
	968	963	7A(6), 7B(120), 10B(11)
		963	7A(120), 10A(11), 7B(6)
928	922	928	7A(56), 8A(12), 9A(7), 13(11), 16(7), 7B(37), 8B(8), 9B(5)
909	909	913	7A(44), 8A(5), 16(6), 7B(73), 8B(8), 9B(6)
886	884	870	7A(18), 18(11), 19(8), 22(11), 23(10), 24 (15)
	846	838	7A(22), 17B(91)
	830	838	7A(91), 7B(22)
		825	7A(6), 8A(8), 23(7), 27(9), 16(12), 7B(16), 8B(18)
792	797	800	11(13), 2A(22), 4A(11), 5A(10), 7A(8), 13(8), 8A(13)
750	757	775	2A(22), 7A(17), 13(12), 8A(22), 21(17), 16(16), 7B(22), 8B(2)
716		699	7A(35), 21(6), 7B(46), 8B(44)
		695	7A(68), 8A(59), 8B(16)
691	699	691	7A(8), 21(26), 5B(7), 7B(58)
	683	674	5A(6), 7A(5), 8A(16), 21(7), 23(9), 14(5), 28(8), 5B(38), 7B(5), 8B(8)
652		638	7A(17), 8A(51), 10(5), 21(6), 27(11), 7B(16), 8B(47)
		625	6B(79)
616	619	620	6A(82)
584	583	576	5A(40), 22(15), 23(7), 8B(8)
509	485	487	5A(13), 13(13), 9A(24), 5B(11), 16(13), 9B(28)
		430	5A(5), 7A(7), 13(26), 9A(74), 21(8), 23(5), 9B(5)
	405	403	16(9), 7B(17), 9B(33), 10B(83)
401		401	7A(27), 10A(136)
	372	399	12(5), 16(12), 7B(17), 9B(41), 10B(74)
307	305	317	12(26), 9A(10), 20(7), 23(27), 24(11)
	263	263	11(7), 12(10), 5A(6), 20(12), 14(11), 15(19), 5B(8)
202	199	222	7A(7), 13(7), 9A(22), 20(60), 24(5), 27(35)
182	186	177	13(8), 9A(11), 21(9), 22(6), 13(21), 16(10), 7B(7), 9B(19)
	130	150	12(13), 20(5), 22(9), 24(14), 27(8), 15(14), 16(13), 9B(8)
106	93	82	13(10), 9A(6), 20(12), 26(32), 27(25), 28(9), 16(12)
61	59	66	12(15), 22(17), 24(36), 15(8), 16(13)
	51	51	13(15), 20(11), 26(12), 27(34), 28(42)
	36	32	13(5), 26(48), 27(5), 28(41)
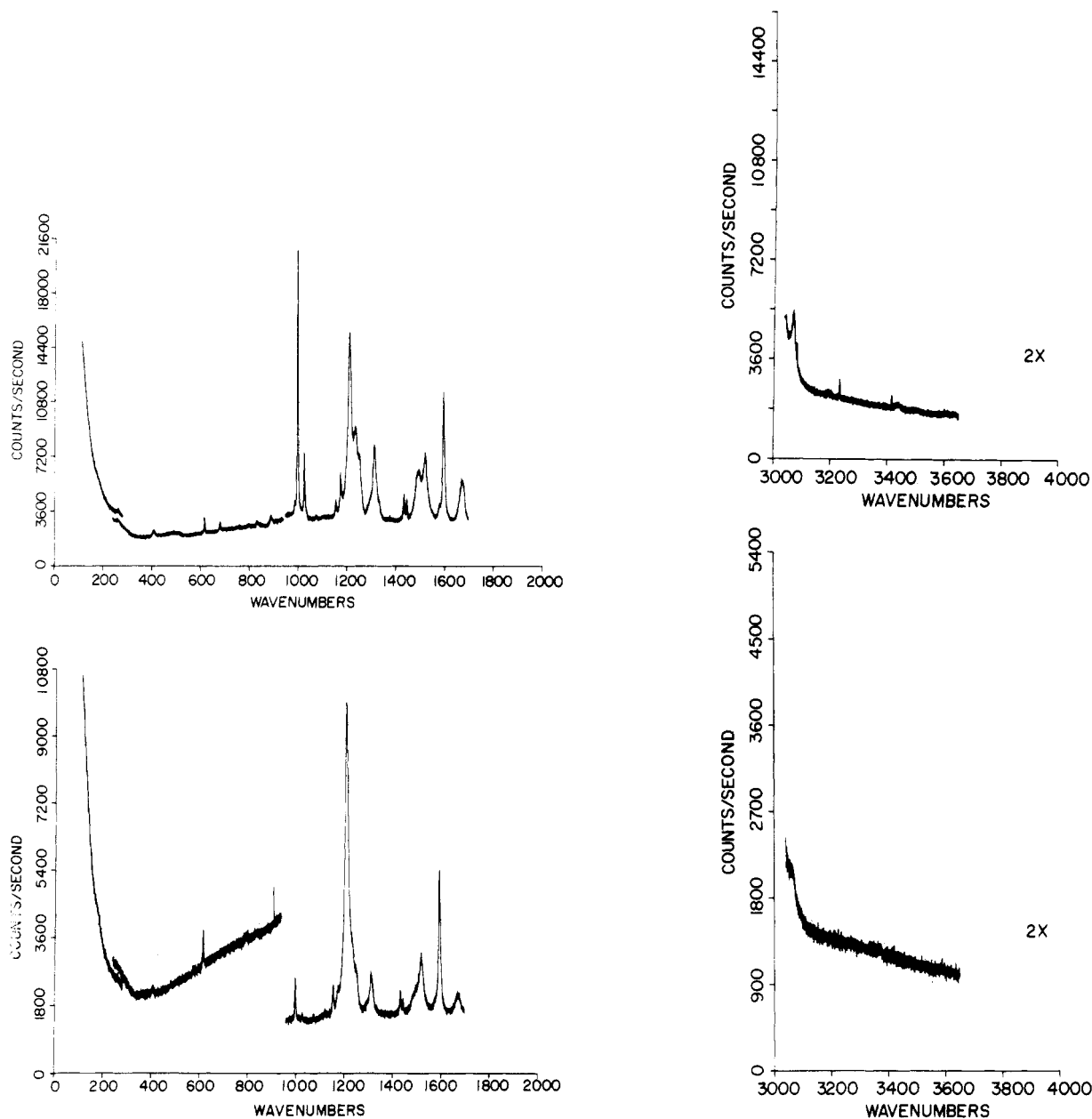
Figure 5. Raman spectra of benzanilide in EtOH solution. Concentration 10% w/w. Incident excitation radiation 5145 Å; 2-cm^{-1} bandpass at 5100 Å. (top left) 0–1700-cm^{-1} region, parallel polarized scattering; (top right) 3000–3600-cm^{-1} region, parallel polarized scattering; (bottom left) 0–1700-cm^{-1} region, perpendicular polarized scattering; (bottom right) 3000–3600-cm^{-1} region, perpendicular polarized.

Results and Discussion

The samples we obtained are comprised of entirely crystalline units. However, the crystallites are small, making polarized infrared spectra impossible to obtain. The observed (both infrared and Raman) and calculated frequencies of both hydrogenated and deuterated benzanilide are tabulated in Table V along with the major contributions to the potential energy distribution (PED) of each mode. The assignments of the calculated bands involving amide group motion are greatly aided by the availability of the deuterated species, –CND–. Furthermore, our results were strongly guided by the experimental and theoretical studies associated with monosubstituted benzenes.[17] This was done under the assumption that most vibrational bands of ring vibrations in substituted benzene would not be significantly affected by the different types of substituents. As expected, the most difficult regions to assign are some of the skeletal vibrations with considerable

mixing of a number of coordinates that exist in the low-frequency region.

Amide group frequencies are usually easy to distinguish from others when NH is exchanged to ND. The strong band at 3345 cm^{-1} in the infrared spectrum is assigned to a mode involving most NH stretching motion. This band shifts down to 2475 cm^{-1} after deuteration, which is slightly higher than the calculated value.

A strong band at 1656 cm^{-1} in both infrared and Raman spectra is assigned to the amide I mode which is dominated by C=O stretching motion, similar to that observed in the polypeptide studies. The strong band at 1536 cm^{-1} in the infrared spectrum is assigned to the amide II mode. The calculated value is in good agreement with the observed frequency. Its PED shows proper contributions from NH in-plane bending, NC(O) stretching, and C=O in-plane bending. In addition, there are considerable contributions from C(O)C stretching and ring CC stretchings. After deuteration, a band of medium intensity is found at 1465
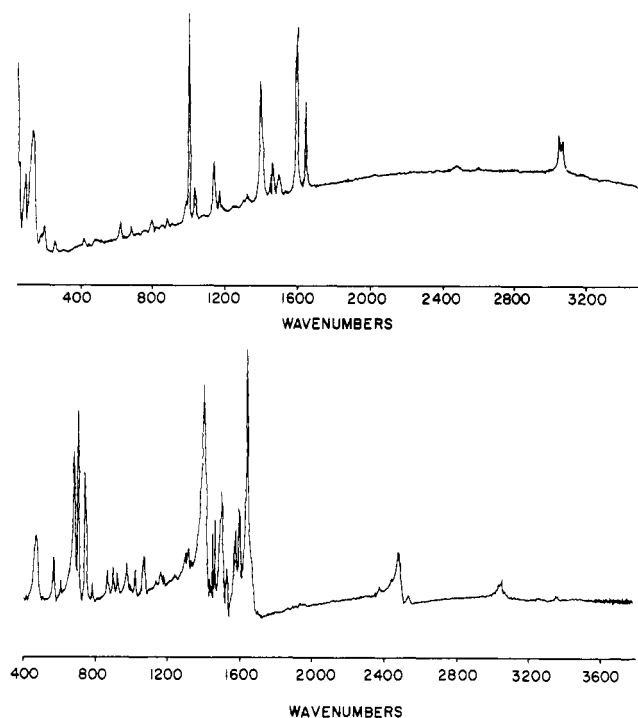
Figure 6. Vibrational difference spectra of deuterated benz-
anilide. (top) Raman spectrum, incident excitation radiation 5145
Å; 2-cm^{-1} bandpass at 5100 Å; (bottom) infrared spectrum, 2-cm^{-1}
resolution. Contributions of the protonated species are digitally
subtracted.

cm^{-1}. The calculated frequency of 1460 cm^{-1} is assigned
to this band on the basis of its PED and comparison with
polypeptide studies where a similar shift in amide II fre-
quency upon deuteration has been observed. Upon deu-
teration its PED changed substantially. For instance, the
ring CC stretching contribution is replaced by contribu-
tions from the ring CH in-plane bending. Bands around
1260 cm^{-1} of medium intensity in both infrared and Raman
spectra are assigned to amide III. This band is generally
regarded as the most sensitive indicator of conformational
change in polypeptides. Its potential energy distribution
is similar to that of amide II except there are greater
contributions from ring in-plane vibrational mode. For
deuterated benzanilide, this band is calculated to be at 959
cm^{-1}. A new band observed near 980 cm^{-1} is therefore
assigned to an amide III like vibrational mode for this
deuterated molecule.

In many synthetic polypeptides, the amide bands are
perturbed by the transition dipole couplings of the hy-
drogen-bonded C=O groups of the adjacent chains.[16]
However, the molecules in the unit cell of benzanilide are
too far apart for such interactions to occur. Therefore,
unlike the multicomponents seen in the spectra of some
polypeptide crystals, we would expect only one nearly
degenerate component for amide bands in either the Ra-
man or infrared spectra obtained.

Since the nonredundant local symmetry coordinates are
well-defined, the assignments of ring vibrations can be
easily accomplished by examining the potential energy
distributions in conjunction with previous studies on
toluene,[17] methyl benzoate,[19] and benzaldehyde.[20] In most
cases, our calculated and observed frequencies showed good
agreement. In the region between 1600 and 1000 cm^{-1}, the
observed bands in both infrared and Raman spectra are
mostly due to ring CC stretching and CH in-plane bending.
Bands near 1502, 1493, 1449, 1440, and 1076 cm^{-1} are due
to ring CC stretching with large contributions from CH
in-plane bending. This type of mixing between these two

internal coordinates has been observed in both benzene
and its monosubstituted derivatives. Furthermore, their
potential energy distributions indicate additional mixing
of vibrational motions between benzene rings. On the
other hand, bands near 1329, 1180, and 1166 cm^{-1} are
mostly due to CH in-plane bending and, finally, bands near
1028 and 1001 cm^{-1} involve CCC valence angle deforma-
tions, i.e., ring in-plane deformations, in addition to either
CH in-plane bending or ring CC stretching. The out-of-
plane bending vibrations are assigned in a similar manner
to the in-plane ones. Again, their frequencies appear to
be characteristic of monosubstituted benzene derivatives
and independent of the type of substitutes. As can be seen
from Table V, the calculated frequencies agree quite well
with those observed. We were curious how the differences
in the environment in the two rings are reflected in the
calculated spectra. The observed band at 1600 cm^{-1} in
both infrared and Raman spectra which is associated with
ring stretching indicates that two phenylene rings in
benzanilide apparently have identical frequencies for this
vibrational mode. This is not reflected in the calculated
spectrum that shows two components at 1606 and 1594
cm^{-1}. This is believed to be directly related to the different
interaction force constants between the ring and the CC(O)
or CN bond stretchings. This apparently was the case for
aromatic polyester as well.[19] In that case, nearly all in-
teraction force constants between the stretching motions
were set to zero in order to reduce the difference calculated.
The main emphasis has been to check the transferability
of the force fields to PPTA and model compounds;
therefore, we did not refine the force field to reduce the
difference between the calculated and experimental values.
It also should be pointed out that this difference in the
local environments of each ring is predicted rather well in
the deuterated molecule. In this case the character of the
mode also changes due to the contribution from the deu-
terated amide groups.

Conclusion

In order to calculate the theoretical vibrational spectra
of molecules possessing a high number of cyclic or
branching redundancies and to minimize the refinement
of the force field needed to describe complicated molecules,
the use of nonredundant symmetry coordinates is perhaps
the most appropriate answer. The use of such a technique
was instrumental in piecing separate force fields together
that had been refined earlier to observe various derivatives
of benzene rings and amide groups in the analysis of
benzanilide. Even though several approaches are available,
we constructed a set of nonredundant symmetry coordi-
nates by incorporating one set that most clearly described
the normal vibrations of rings to other coordinates com-
monly used to describe the amide vibration. Even though
this approach is not easily carried out entirely by computer,
and it in fact may not be generally applicable to all mol-
ecules, in this particular case when reliable force fields are
available from other means, satisfactory results were ob-
tained for this model compound without any need for
force-field refinement. We have carried out similar studies
for poly(p-phenylene terephthalate). The results of that
calculation will be published in a subsequent paper.

References and Notes

(1) Haraguchi, K.; Kajiyama, T.; Takayangi, M. *J. Appl. Polym. Sci.* **1979**, *23*, 903.
(2) Haraguchi, K.; Kajiyama, T.; Takayanagi, M. *J. Appl Polym. Sci.* **1979**, *23*, 915.
(3) Morgan, P. W. *Macromolecules* **1977**, *10*, 1381.
(4) Kwolek, S. L.; Morgan, P. W.; Schaefgen, J. R.; Gulrich, L. W. *Macromolecules* **1977**, *10*, 1390.
(5) Tashiro, K.; Kobayashi, M.; Tadokoro, H. *Macromolecules* **1977**, *10*, 413.
(6) Northolt, M. G.; van Aartsen, J. J. *J. Polym. Sci.; Appl. Polym. Symp.* **1977**, *58*, 283.
(7) Shen, D. Y.; Hsu, S. L. *Polymer* **1982**, *23*, 969.
(8) Penn, L.; Milanovich, F. *Polymer* **1979**, *20*, 31.
(9) Penn, L.; Larsen, F. *J. Appl. Polym. Sci.* **1979**, *23*, 59.
(10) Pulay, P.; Fogarasi, G.; Boggs, J. E. *J. Chem. Phys.* **1981**, *74*, 3999.
(11) Dwivedi, A.; Krimm, S. *Macromolecules* **1982**, *15*, 177.
(12) Northolt, M. G. *Eur. Polym. J.* **1974**, *10*, 799.
(13) Kashino, S.; Ito, K.; Haisa, M. *Bull. Chem. Soc. Jpn.* **1979**, *52*(2), 365.
(14) Gussoni, M.; Zerbi, G. *Atti. Accad. Naz. Lincei* **1966**, *40*, 1032.
(15) Cheam, T. Ph.D. Thesis, University of Michigan, 1983.
(16) Abe, Y.; Krimm, S. *Biopolymers* **1972** *11*, 1817.
(17) La Lau, C.; Snyder, R. G. *Spectrochim. Acta, Part A* **1971**, *27* 2073.
(18) Schachtschneider, J. H.; Snyder, R. G. *Spectrochim. Acta* **1963**, *19*, 117.
(19) Boerio, F. J.; Bahl, S. K. *Spectrochim. Acta, Part A* **1976**, *32*, 987.
(20) Zwarich, R.; Smolarek, J.; Goodman, L. *J. Mol. Spectrosc.* **1971**, *38*, 336.